Two-Photon Exchange in Electron-Proton Scattering*

GARY K. GREENHUT†
Laboratory of Nuclear Studies, Cornell University, Ithaca, New York 14850
(Received 25 February 1969)

An investigation is made of the two-photon exchange contribution to e-p scattering. The contribution is calculated in second Born approximation using potentials representing the charge and magnetic moment distributions of the proton. A fit to proton Compton scattering data is made and used to calculate the resonance contribution to e-p scattering. At high energies, the resonant and nonresonant contributions to the two-photon exchange effect tend to cancel one another.

I. INTRODUCTION

THE validity of the form-factor analysis of electron-proton scattering[1] is based on the assumption that the contribution of the two-photon exchange amplitude (Fig. 1) is negligibly small. Experimentally, the real part of this amplitude is obtained by comparing electron-proton and positron-proton scattering at the same energy and angle.[2] The cross sections are observed to be equal, to within 1 or 2 standard deviations, up to incident laboratory energies of 10 GeV and squared momentum transfers of 5 $(\text{GeV}/c)^2$.

The theoretical analyses of the two-photon amplitude can be separated into two classes. In the case of unexcited intermediate proton states, the calculations are done using static-charge distributions.[3,4] When compared with lowest order, these calculations are of the order of the fine-structure constant α, never exceeding a few percent. In the case of excited intermediate proton states, results have been obtained for the contribution if the $\Delta(1236)$ resonance in the s channel[5–8] and for $J^{PC}=1^{++}$ [9] and 2^{++} [10] meson exchange in the s channel. These results never exceed a few percent of the lowest-order cross section.

In this paper, we look again at the problem of predicting the two-photon exchange effect in e-p scattering. The two-photon effect is largest in the backward direction where the scattering is dominated by the magnetic moment distribution. In Sec. II, the magnetic moment distribution is introduced into the static-potential calculation in order to improve the estimate of the two-photon exchange effect for scattering into backward angles. In Sec. III a phenomenological fit to proton Compton scattering data is made and used in Sec. IV to calculate s-channel resonance contributions to e-p scattering. The results are compared with those obtained previously by other authors. Finally, in Sec. V, the contributions to the two-photon exchange effect are summarized and compared with the experimental data.

II. UNEXCITED INTERMEDIATE PROTON STATES

The potentials necessary for a static calculation of the two-photon exchange effect are obtained from the lowest-order proton current[11]

$$\begin{aligned}\bar{u}(P_f)\Gamma_\mu u(P_i) &= \bar{u}(P_f)\left[\gamma_\mu F_1(Q^2)+i\frac{\sigma_{\mu\nu}Q^\nu}{2M}\kappa F_2(Q^2)\right]u(P_i)\\ &= \bar{u}(P_f)\left[\frac{P_i+P_f}{2M}F_1(Q^2)+\frac{i\sigma_{\mu\nu}Q^\nu}{2M}G_M(Q^2)\right]u(P_i)\,, \quad (2.1)\end{aligned}$$

where P_i and P_f are the initial and final momenta of the proton, κ is the anomalous magnetic moment, F_1, F_2, and G_M are the usual proton form factors, and

$$Q=P_f-P_i. \quad (2.2)$$

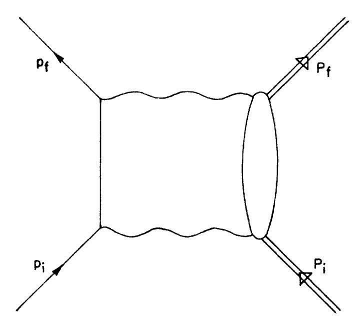

FIG. 1. Two-photon exchange in e-p scattering.

* Supported in part by the U. S. Office of Naval Research.
† Present address: Department of Physics, Northeastern University, Boston, Mass.
[1] M. Rosenbluth, Phys. Rev. **79**, 615 (1950.)
[2] A compilation of the results of these experiments up to the present is given by Mar *et al.*, Phys. Rev. Letters **21**, 482 (1968).
[3] R. R. Lewis, Phys. Rev. **102**, 537 (1956). This paper discusses the Coulomb, Yukawa, exponential, and Gaussian charge distributions.
[4] Numerical calculations for Coulomb and Yukawa charge distributions can be found in P. Budini and G. Furlan, Nuovo Cimento **13**, 790 (1959); G. Bisiacchi and G. Furlan, Phys. Letters **3**, 186 (1963).
[5] S. D. Drell and M. A. Ruderman, Phys. Rev. **106**, 561 (1967).
[6] S. D. Drell and S. Fubini, Phys. Rev. **113**, 741 (1959).
[7] N. R. Werthamer and M. A. Ruderman, Phys. Rev. **123**, 1005 (1961).
[8] J. A. Campbell, Nucl. Phys. **B1**, 283 (1967).
[9] S. D. Drell and J. D. Sullivan, Phys. Letters **19**, 516 (1965); M. Gourdin, *Diffusion des Électrons de Haute Énergie* (Masson et Cie., Paris, 1966).
[10] D. Flamm and W. Kummer, Nuovo Cimento **28**, 33 (1963).
[11] We use $\hbar=c=1$ and the notation of J. D. Bjorken and S. D. Drell, *Relativistic Quantum Mechanics* (McGraw-Hill Book Co., New York, 1964).

To order $1/M$, Eq. (2.1) is given by

$$\bar{u}(P_f)\Gamma^0 u(P_i)\cong F_1(Q^2)\varphi_f{}^\dagger\varphi_i\,, \tag{2.3a}$$

$$\bar{u}(P_f)\Gamma^j u(P_i)\cong\frac{(P_i+P_f)^j}{2M}F_1(Q^2)\varphi_f{}^\dagger\varphi_i - \frac{i}{2M}(1+\kappa)\epsilon^{jkl}(\sigma_p)_l Q_k F_m(Q^2)\,, \tag{2.3b}$$

where

$$F_m(Q^2)=G_M(Q^2)/(1+\kappa)$$

and

$$(\sigma_p)_l=\varphi_f{}^\dagger\sigma_l\varphi_i\,,$$

the φ functions being the two-component Pauli spinors for the proton.

It is known from the work on the effective-potential approach to the electron-proton interaction[12] that, in the case of charge distribution scattering, where the potential is obtained from (2.3a), a static calculation of the cross section without proton recoil gives the correct c.m. result with recoil to order E/M, where E is the energy, if the static-frame energy and scattering angle are identified as c.m. quantities. This is not true for magnetic moment distribution scattering which arises from the second term on the right-hand side of (2.3b). In this case, in order to relate the static calculation to c.m. scattering with recoil, a factor M/W must be included, where

$$W=E+(E^2+M^2)^{1/2} \tag{2.4}$$

is the total c.m. energy. The result is that the following momentum-space potentials shall be used:

$$A_0=[F_1(Q^2)/\mathbf{Q}^2]\varphi_f{}^\dagger\varphi_i\,, \tag{2.5a}$$

$$A_l=-(i/2W)(1+\kappa)\epsilon_{lkj}(\sigma_p)^k Q^j F_m(Q^2)/\mathbf{Q}^2\,, \tag{2.5b}$$

without proton recoil, with the provision that the energies and angles be identified as c.m. quantities. The static calculations are valid only for c.m. energies less than the proton mass. However, we will show results at somewhat higher energies to indicate the expected trend.

To lowest order, the potentials (2.5) give the following cross section:

$$\frac{d\sigma}{d\Omega}=\sigma_M\left[F_1{}^2(Q^2)+\frac{\mathbf{Q}^2}{4W^2}G_M{}^2(Q^2)+\frac{\mathbf{Q}^2}{2W^2}G_M{}^2(Q^2)\tan^2(\tfrac{1}{2}\theta)\right], \tag{2.6}$$

where

$$\sigma_M=\alpha^2\cos^2(\tfrac{1}{2}\theta)/4E^2\sin^4(\tfrac{1}{2}\theta)$$

and

$$\mathbf{Q}^2=4E^2\sin^2(\tfrac{1}{2}\theta)\,.$$

[12] H. Grotch and D. R. Yennie, Z. Physik **202**, 425 (1967).

In the forward and backward directions, (2.6) agrees with the correct lowest-order c.m. cross section with recoil

$$\frac{d\sigma^{(1)}}{d\Omega}=\sigma_M\left[F_1{}^2(Q^2)+\frac{\mathbf{Q}^2}{4M^2}\kappa^2F_2{}^2(Q^2)+\frac{\mathbf{Q}^2}{2W^2}G_M{}^2(Q^2)\tan^2(\tfrac{1}{2}\theta)\right] \tag{2.7}$$

obtained from (2.1). In all comparisons with lowest order, we shall use (2.7).

To order α^3, the e-p scattering cross section can be written

$$\frac{d\sigma}{d\Omega}=\frac{d\sigma^{(1)}}{d\Omega}+\sum\left(\frac{d\sigma^{(2)}}{d\Omega_{a,bc}}\right), \tag{2.8}$$

where $(d\sigma^{(2)}/d\Omega)_{a,bc}$ arises from the cross term between the first- and second-order Born-approximation amplitudes. If p_i and p_f are the initial and final momenta of the electron, we then define

$$\mathbf{Q}=\mathbf{p}_i-\mathbf{p}_f,\qquad \mathbf{P}=\mathbf{p}_i+\mathbf{p}_f\,,$$
$$\mathbf{Q}^2=4E^2\sin^2(\tfrac{1}{2}\theta),\quad \mathbf{P}^2=4E^2\cos^2(\tfrac{1}{2}\theta)\,,$$

and obtain the following results for the α^3 contribution to (2.8) in second Born approximation:

$$\left(\frac{d\sigma^{(2)}}{d\Omega}\right)_{e,ee}=\sigma_M\frac{\alpha}{\pi^2}\frac{E\mathbf{Q}^2}{\mathbf{P}^2}F_1(Q^2)(\mathrm{Re}I_{e,ee})\,,$$

$$I_{e,ee}=\int d^3q\frac{(\mathbf{P}^2+2\mathbf{P}\cdot\mathbf{q})}{\mathbf{q}^2-E^2-i\epsilon}\frac{F_1(|\mathbf{q}-\mathbf{p}_f|^2)}{|\mathbf{q}-\mathbf{p}_f|^2}\times\frac{F_1(|\mathbf{q}-\mathbf{p}_i|^2)}{|\mathbf{q}-\mathbf{p}_i|^2}; \tag{2.9}$$

$$\left(\frac{d\sigma^{(2)}}{d\Omega}\right)_{a,bc}=\sigma_M\frac{\alpha}{\pi^2}\frac{E\mathbf{Q}^2}{\mathbf{P}^2}\frac{\mathbf{Q}^2}{2W^2}(1+\kappa)^2F_m(Q^2)(\mathrm{Re}I_{a,bc})\,,$$

$$I_{a,bc}=\frac{1}{4\mathbf{Q}^2}\int d^3q\frac{\beta_{a,bc}}{\mathbf{q}^2-E^2-i\epsilon}\frac{F_c(|\mathbf{q}-\mathbf{p}_f|^2)}{|\mathbf{q}-\mathbf{p}_f|^2}\times\frac{F_b(|\mathbf{q}-\mathbf{p}_i|^2)}{|\mathbf{q}-\mathbf{p}_i|^2} \tag{2.10}$$

(at least one of $a,b,c=m$);

$$\beta_{e,mm}=[F_1(Q^2)/F_m(Q^2)][\mathbf{P}^4-4\mathbf{P}^2(\mathbf{q}\cdot\mathbf{P})-8E^2(\mathbf{q}\cdot\mathbf{P})+8\mathbf{P}^2\mathbf{q}^2+4(\mathbf{q}\cdot\mathbf{P})^2-8\mathbf{q}^2(\mathbf{q}\cdot\mathbf{P})]\,,$$

$$\beta_{m,me}=\beta_{m,em}=4E^2\mathbf{Q}^2+\mathbf{Q}^4+4(\mathbf{q}\cdot\mathbf{Q})^2+4\mathbf{q}^2\mathbf{Q}^2-16E^2(\mathbf{q}\cdot\mathbf{Q})-4\mathbf{Q}^2(\mathbf{q}\cdot\mathbf{Q})\,,$$

$$\beta_{m,mm}=[(1+\kappa)/EW][-2E^2\mathbf{P}^2\mathbf{Q}^2-12E^2\mathbf{Q}^2\mathbf{q}^2+10E^2\mathbf{Q}^2(\mathbf{q}\cdot\mathbf{P})+2\mathbf{Q}^2\mathbf{q}^2(\mathbf{q}\cdot\mathbf{P})-\mathbf{Q}^2(\mathbf{q}\cdot\mathbf{P})^2+8E^2(\mathbf{q}\cdot\mathbf{Q})^2+\mathbf{Q}^2(\mathbf{q}\cdot\mathbf{Q})^2]\,.$$

Defining σ_+ (σ_-) to be differential positron (electron) scattering cross section, then

$$\frac{\sigma_+}{\sigma_-}-1=-2\left[\sum\left(\frac{d\sigma^{(2)}}{d\Omega}\right)_{a,bc}\bigg/\frac{d\sigma^{(1)}}{d\Omega}\right]=\frac{F_1{}^2(Q^2)(\sigma_+/\sigma_--1)_e+(\mathbf{Q}^2/2W^2)G_M{}^2(Q^2)\tan^2(\frac{1}{2}\theta)(\sigma_+/\sigma_--1)_m}{F_1{}^2(Q^2)+(\mathbf{Q}^2/4M^2(\kappa^2F_2{}^2(Q^2)+(\mathbf{Q}^2/2W^2)G_M{}^2(Q^2)\tan^2(\frac{1}{2}\theta)}, \quad (2.11)$$

where

$$\left(\frac{\sigma_+}{\sigma_-}-1\right)_e=-\frac{2\alpha}{\pi^2}\frac{E\mathbf{Q}^2}{\mathbf{P}^2}\frac{1}{F_1(Q^2)}(\mathrm{Re}\, I_{e,ee}),$$

$$\left(\frac{\sigma_+}{\sigma_-}-1\right)_m=-\frac{2\alpha}{\pi^2}E\frac{1}{F_m(Q^2)}[\mathrm{Re}\,(I_{e,mm}+I_{m,me}+I_{m,em}+I_{m,mm})].$$

For simplicity, (2.9)–(2.11) are evaluated using Yukawa form factors

$$F_1(Q^2)=F_m(Q^2)=a^2/(a^2+\mathbf{Q}^2), \quad (2.12)$$

with $a=600$ MeV corresponding to an rms radius of 0.8 F. Using a partial fraction decomposition, the resulting integrals are similar to those evaluated in Ref. 3. The details are given elsewhere.[13] The results for a c.m. energy of 850 MeV, corresponding to an incident laboratory energy of 1.9 GeV, are shown in Fig. 2, where θ is the c.m. scattering angle. The result in Fig. 2(a) corresponds to the calculation of Lewis[3] where only the proton charge distribution is taken into account. It is seen in Fig. 2(c) that including the magnetic moment distribution decreases the size of the two-photon exchange effect in the backward direction. Results for σ_+/σ_--1 are shown for various c.m. energies in Fig. 3 and the variation of the effect at $\theta=180°$ is shown in Fig. 4. At fixed Q^2, the second Born approximation for σ_+/σ_--1 goes as $1/E$ for large energies.

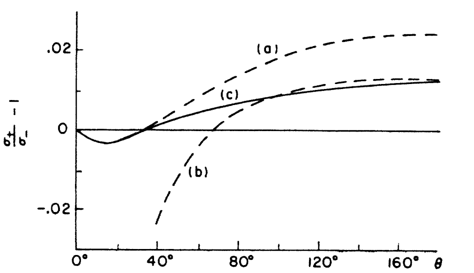

FIG. 2. Second Born approximation at $E=850$ MeV. (a) $(\sigma_+/\sigma_--1)_e$; (b) $(\sigma_+/\sigma_--1)_m$; (c) σ_+/σ_--1.

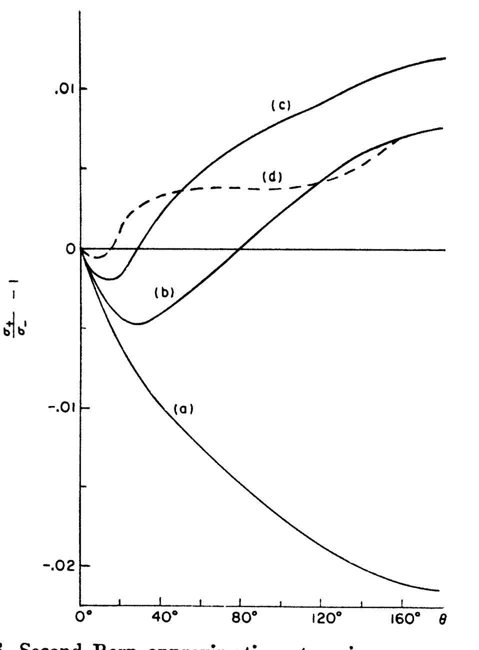

FIG. 3. Second Born approximation at various c.m. energies. (a) $E=200$ MeV, (b) $E=500$ MeV, (c) $E=1000$ MeV, (d) $E=2000$ MeV.

A calculation of the two-photon exchange effect using the potentials in (2.5) has been done[13] using the distorted-wave approximation.[14] We do not give the details here but remark that the results agree well with those obtained above using the second Born approximation. This indicates that the physical picture associated with the distorted-wave method is a good approximation to the physical processes underlying the higher-order corrections to the Born approximation. This physical picture is as follows: The electron wave function, initially a plane wave, is gradually distorted by a succession of small momentum transfers from the

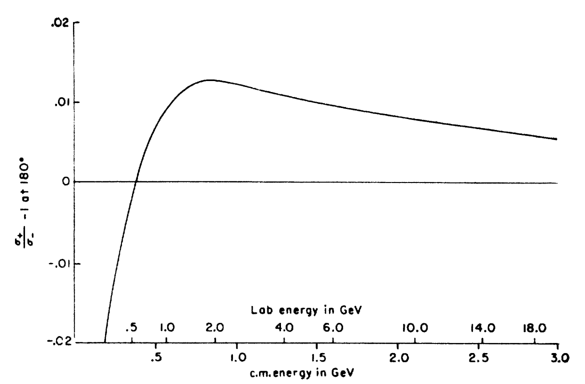

FIG. 4. Second Born approximation at 180°.

[13] G. K. Greenhut, Ph.D. thesis, Cornell University, 1968 (unpublished).

[14] D. R. Yennie, F. L. Boos, and D. G. Ravenhall, Phys. Rev. 137, B882 (1965).

target. The electron then receives one large transfer of momentum in the vicinity of the target, giving rise to the main scattering. The scattered wave continues to be distorted by another succession of small momentum transfers.

We can use the distorted-wave picture to understand the general shape of the curves in Figs. 2 and 3. The electron wave function is focused toward the center of the potential, decreasing its effective impact parameter. The reverse occurs for positrons. For low momentum transfers, at a given energy and angle, electron scattering dominates positron scattering. At high momentum transfers, the fact that the proton charge and magnetic moment distributions are extended becomes important. Since the electron wave function is focused toward the center of the distributions, the electron experiences less effective charge than the positron and therefore at high momentum transfers, positron scattering dominates electron scattering. From the point of view of momentum space, the wave distortion causes the wave number of the electron to be enhanced. The form factor is therefore evaluated at a larger momentum transfer for electrons than for positrons.

It should be pointed out that contributions to the scattering amplitude of order α^2 and E/M are also present in the radiative corrections, the dominant portion coming from the infrared-divergent parts. These contributions have presumably been included in the analysis of the experimental data.

III. PROTON COMPTON SCATTERING

In order to calculate the resonance contribution to the two-photon exchange effect, the proton Compton scattering amplitude for off-mass-shell photons is needed. A previous calculation of the resonance contribution[8] used the model of Gourdin and Salin[15] to obtain the contribution of the $\Delta(1236)$ to the two-photon effect. In this work, we use a simplified version of the proton Compton scattering amplitude[16] consisting of the proton Born terms with the correct low-energy limit,[17] π^0 and η^0 pole terms, and crossing-symmetric Breit-Wigner resonance terms representing the proton s-channel resonances. The diagrams corresponding to the Born and pole terms are shown in Fig. 5. The experimental values are used for the π^0 and η^0 couplings. One free-coupling parameter is used in each of the Breit-Wigner terms. The values of these parameters are determined by a fit to the proton Compton scattering data.

The S matrix for Compton scattering in the c.m. system is given by

$$S=ie^2(2\pi)^4\delta^4(k+P_i-k'-P_f)(M/\omega\mathcal{E})T_C,$$

where k and k' are the initial and final photon momenta with energy component ω, and P_i and P_f are the initial and final proton momenta with energy component $\mathcal{E}$. In the c.m. frame

$$T_C=R_1(\mathbf{e}\cdot\mathbf{e}')+\frac{R_2}{\omega^2}[(\mathbf{k}\times\mathbf{e})\cdot(\mathbf{k}'\times\mathbf{e}')]+iR_3[\boldsymbol{\sigma}\cdot(\mathbf{e}'\times\mathbf{e})]+i\frac{R_4}{\omega^2}\{\boldsymbol{\sigma}\cdot[(\mathbf{k}'\times\mathbf{e}')\times(\mathbf{k}\times\mathbf{e})]\}$$
$$+i\frac{R_5}{\omega^2}\{(\boldsymbol{\sigma}\cdot\mathbf{k})[\mathbf{k}'\cdot(\mathbf{e}'\times\mathbf{e})]-(\boldsymbol{\sigma}\cdot\mathbf{k}')[\mathbf{k}\cdot(\mathbf{e}\times\mathbf{e}')]\}+i\frac{R_6}{\omega^2}\{\boldsymbol{\sigma}(\cdot\mathbf{k}')[\mathbf{k}'\cdot(\mathbf{e}'\times\mathbf{e})]-(\boldsymbol{\sigma}\cdot\mathbf{k})[\mathbf{k}\cdot(\mathbf{e}\times\mathbf{e}')]\},\quad(3.1)$$

$$\frac{d\sigma}{d\Omega_C}=\frac{\alpha^2M^2}{V^2}[\tfrac{1}{2}(1+x^2)(|R_1|^2+|R_2|^2)+\tfrac{1}{2}(3-x^2)(|R_3|^2+|R_4|^2)+(1+3x^2)(|R_5|^2+|R_6|^2)$$
$$+2(1+x^2)\,\mathrm{Re}(R_4R_5^*+R_3R_6^*)+2x\,\mathrm{Re}(R_1R_2^*+R_3R_4^*+2R_3R_5^*+2R_4R_6^*)+2x(3+x^2)\,\mathrm{Re}(R_5R_6^*)],\quad(3.2)$$

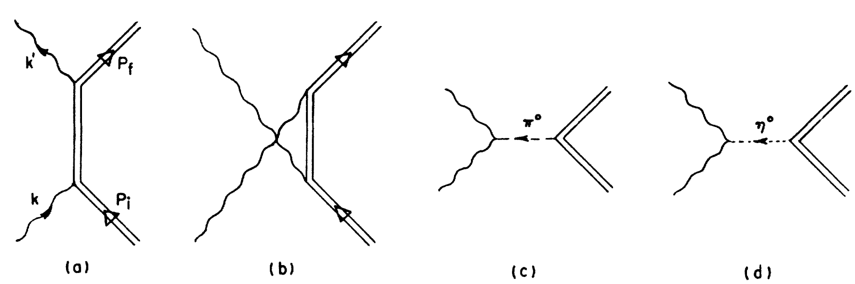

FIG. 5. One-particle intermediate states in proton Compton scattering. (a) and (b) Born terms, (c) π^0 pole term, (d) η^0 pole term.

[15] M. Gourdin and P. Salin, Nuovo Cimento **27**, 193 (1963); **27**, 309 (1963).
[16] Y. Nagashima, Progr. Theoret. Phys. (Kyoto) **33**, 828 (1965).
[17] M. Gell-Mann and M. L. Goldberger, Phys. Rev. **96**, 1433 (1954); F. E. Low, *ibid.* **96**, 1428 (1954).

where $x=\cos\theta^*$, θ^* being the c.m. scattering angle, and V is the total c.m. energy

$$V=\omega+(M^2+\omega^2)^{1/2}=\omega+\mathcal{E}.$$

The scalar functions in (3.1) are decomposed as follows:

$$R_i=R_i^B+R_i^L+R_i^r, \qquad (3.3)$$

where R_i^B is the proton Born-term contribution, R_i^L is the combined contribution of the π^0 and η^0 pole terms, and R_i^r is the combined contribution of the proton s-channel resonance terms.

The Born-term contributions are[18]

$$R_1^B=-\frac{\mathcal{E}+M-(\mathcal{E}-M)x}{2M(1-x^2)}(A_3+xA_1) -\frac{(\mathcal{E}+M)(V-M)+(\mathcal{E}-M)(V+M)x}{4M^2(1-x^2)}(A_4+xA_2),$$

$$R_2^B=-R_1^B \text{ (with } A_3\leftrightarrow A_1,\ A_4\leftrightarrow A_2),$$

$$R_3^B=-\frac{\mathcal{E}-M}{2M}\left(A_1-\frac{V+M}{2M}A_2\right), \qquad (3.4)$$

$$R_4^B=-R_3^B \text{ (with } A_1\leftrightarrow A_3,\ A_2\leftrightarrow A_4),$$

$$R_5^B=\frac{\mathcal{E}-M}{2M(1-x^2)}\left[-A_3+\frac{V+M}{2M}A_4 -\left(A_1-\frac{V+M}{2M}A_2\right)x\right]-\frac{\omega V}{8M^2(1+x)}A_5 +\frac{\omega}{4M(1-x)}A_6,$$

$$R_6^B=-R_5^B \text{ (with } A_3\leftrightarrow A_1,\ A_4\leftrightarrow A_2,\ A_6\leftrightarrow -A_6),$$

where

$$A_1=-2M[1/(M^2-s)+1/(M^2-u)],$$
$$A_2=-2M[1/(M^2-s)-1/(M^2-u)],$$
$$A_3=-[1-(1+\kappa)^2]/M,$$
$$A_4=2M(1+\kappa)^2[1/(M^2-s)-1/(M^2-u)],$$
$$A_5=-4M(1+\kappa)[1/(M^2-s)+1/(M^2-u)]-2\kappa^2/M,$$
$$A_6=2M(1+\kappa)[1/(M^2-s)+1/(M^2-u)] +[(1+\kappa)^2-1]/M,$$
$$s=V^2,\quad t=-2\omega^2(1-x),\quad u=2M^2-V^2+2\omega^2(1-x).$$

For the pole-term contribution, the standard π-N coupling is used at the proton vertex and the following coupling is used at the photon vertex:

$$-f\epsilon^{\mu\nu\alpha\beta}b_\mu(k+k')_\nu e_\alpha e_\beta',$$

where e and e' are the polarization four-vectors of the incoming and outgoing photons, b is the momentum carried by the intermediate particle [as in Figs. 5(c) and 5(d)], and

$$f^2/4\pi=4/m^2(m\tau),$$

where m is the mass of the exchanged meson and τ its lifetime for decay into two photons. The contribution of π^0 and η^0 exchange to (3.1) can then be written[16]

$$R_1^L=R_2^L=R_3^L=R_4^L=0,$$

$$R_5^L=-\frac{1}{\alpha}\frac{k}{M}\left[\left(\frac{g_\pi^2}{4\pi}\right)^{1/2}\frac{1}{m_\pi(m_\pi\tau_\pi)^{1/2}}\frac{1}{1-x+m_\pi^2/2\omega^2} +\left(\frac{g_\eta^2}{4\pi}\right)^{1/2}\frac{1}{m_\eta(m_\eta\tau_\eta)^{1/2}}\frac{1}{1-x+m_\eta^2/2\omega^2}\right], \qquad (3.5)$$

$$R_6^L=-R_5^L.$$

The constants in (3.5) are given in Table I.[19]

We now turn to the proton s-channel resonances. We shall consider only those resonances with masses less than 1700 MeV, since above this energy the data[20] begin to show a rapid decrease with increasing energy. This behavior cannot be easily fitted with Born terms, t-channel exchange terms, and Breit-Wigner resonance terms. We also restrict our attention to resonances with elasticities into the π-N channel of greater than 50%. This reduces the number of resonances of interest to four: the $\Delta(1236)$, $N(1400)$, $N(1525)$, and $N(1688)$. The masses (M_i^*), widths (Γ_{0i}), orbital angular momenta (L), spins (J), parities (P), and isotropic spins (I) of these resonances are given in Table II.

A partial-wave decomposition of the Compton scattering amplitude in the c.m. system gives the following result for the scalar functions in (3.1) [18]:

$$R_1=\sum_{l=1}^{\infty}\{[(l+1)f_{EE}^{l+}+lf_{EE}^{l-}](P_l'+xP_l'') -[(l+1)f_{MM}^{l+}+lf_{MM}^{l-}]P_l''\},$$

$$R_2=R_1 \text{ (with } E\leftrightarrow M),$$

$$R_3=\sum_{l=1}^{\infty}\{(f_{EE}^{l+}-f_{EE}^{l-})[-P_l'-3xPl''+(1-x^2)P_l'''] -(f_{MM}^{l+}-f_{MM}^{l-})P_l''+f_{EM}^{l-}[(l-1)P_l'-xP_l''] +(f_{ME}^{l-}-f_{ME}^{l+})P_l''+f_{EM}^{l+}[(l+2)P_l'\times xP_l'')\},$$

TABLE I. Parameters for the π^0 and η^0 amplitudes.

	$g^2/4\pi$	m (MeV)	τ (sec)
π^0	14	135	0.89×10^{-16}
η^0	8	549	0.54×10^{-18}

[18] A. P. Contogouris, Nuovo Cimento **25**, 104 (1962).

[19] We use the η-ρ coupling determined by J. S. Ball [Phys. Rev. **149**, 1191 (1966)] and the η lifetime from the experiment of C. Bemporad *et al.* [Phys. Letters **25B**, 380 (1967)].

[20] M. Deutsch *et al.*, in *Proceedings of the 1967 International Symposium on Electron and Photon Interactions at High Energies* (Stanford Linear Accelerator Center, Stanford, Calif., 1968), p. 619.

TABLE II. Parameters associated with the proton resonances.

i	Resonance	M_i^* (MeV)	Γ_{0i} (MeV)	$L_{2I,2J}^P$	Dominant partial-wave amplitude	ω_i (MeV)	ω_i^{lab} (MeV)	h_i (MeV)	C_i
1	$\Delta(1236)$	1236	120	P_{33}^+	f_{MM}^{1+}	262	346	231	0.46
2	$N(1400)$	1400	200	P_{11}^+	f_{MM}^{1-}	386	578	367	0.35
3	$N(1525)$	1525	105	D_{13}^-	f_{EE}^{1+}	474	771	460	0.55
4	$N(1688)$	1688	110	F_{15}^+	f_{EE}^{2+}	584	1050	573	0.10

$R_4=R_3$ (with $E\leftrightarrow M$),

$$R_5=\sum_{l=1}^{\infty}\{(f_{EE}^{l+}-f_{EE}^{l-})(2P_l''+P_l''')-(f_{MM}^{l+}-f_{MM}^{l-})P_l''' +\tfrac{1}{2}f_{EM}^{l-}[(l-4)P_l''-2xP_l'''] +\tfrac{1}{2}f_{ME}^{l-}[2(1-l)P_l'+(4-l)xP_l''+(1+x^2)P_l'''] -\tfrac{1}{2}f_{ME}^{l+}[2(l+2)P_l'+(l+5)P_l''+(x^2+1)P^{l'''}) +\tfrac{1}{2}f_{EM}^{l+}[(l+5)P_l''+2xP_l''']\}, \quad (3.6)$$

$R_6=R_5$ (with $E\leftrightarrow M$),

where $P_l^{(n)}\equiv(d/dx)^nP_l(x)$, P_l being the lth-order Legendre polynomial, and $f_{EE}^{l\pm}$ is the partial-wave amplitude for the transition. $|j=l\pm\frac{1}{2}, E, l\rangle\rightarrow|j=l\pm\frac{1}{2}, E, l\rangle$ and similarly for $f_{MM}^{l\pm}$, $f_{EM}^{l\pm}$, and $f_{ME}^{l\pm}$. E and M denote an electric and a magnetic multipole state, respectively. We shall retain only the dominant partial-wave amplitude for each resonance. These are given in Table II. Decomposing the resonance contribution to the scalar amplitudes as follows:

$$R_i^r=R_i^{(1)}+R_i^{(2)}+R_i^{(3)}+R_i^{(4)}, \quad (3.7)$$

and using (3.6), we obtain

for $\Delta(1236)$:

$$R_1^{(1)}=R_3^{(1)}=R_5^{(1)}=R_6^{(1)}=0,$$
$$R_2^{(1)}=2f_{MM}^{1+},\quad R_4^{(1)}=-\hat{f}_{MM}^{1+};$$

for $N(1400)$:

$$R_1^{(2)}=R_3^{(2)}=R_5^{(2)}=R_6^{(2)}=0,$$
$$R_2^{(2)}=f_{MM}^{1-},\quad R_4^{(2)}=\hat{f}_{MM}^{1-}; \quad (3.8)$$

for $N(1525)$:

$$R_1^{(3)}=2f_{EE}^{1+},\quad R_3^{(3)}=-\hat{f}_{EE}^{1+},$$
$$R_2^{(3)}=R_4^{(3)}=R_5^{(3)}=R_6^{(3)}=0;$$

for $N(1688)$:

$$R_1^{(4)}=18f_{EE}^{2+},\quad R_2^{(4)}=-9f_{EE}^{2+},\quad R_3^{(4)}=-12\hat{f}_{EE}^{2+},$$
$$R_4^{(4)}=-3\hat{f}_{EE}^{2+},\quad R_5^{(4)}=6\hat{f}_{EE}^{2+},\quad R_6^{(4)}=0.$$

Crossing symmetry requires that the following relations hold at $x=-1$:

$$R_1(\omega)-R_2(\omega)=R_1(-\omega)-R_2(-\omega),$$
$$R_3(\omega)-R_4(\omega)-2R_5(\omega)+2R_6(\omega) =-[R_3(-\omega)-R_4(-\omega)-2R_5(-\omega)+2R_6(-\omega)].$$

We have distinguished between the amplitudes associated with R_1 and R_2 and with R_3–R_6 in (3.8), the latter having a caret, because of their different behavior under crossing.

Redefining the partial-wave amplitudes

$$f_1\equiv f_{MM}^{1+},\quad f_2\equiv f_{MM}^{1-},\quad f_3\equiv f_{EE}^{1+},\quad f_4\equiv f_{EE}^{2+},$$

and similarly for the careted amplitudes, the amplitudes are given the following crossing-symmetric Breit-Wigner form:

$$f_i=\frac{C_i}{|\omega|}\tfrac{1}{2}\Gamma_i\left[\frac{1}{\omega-\omega_i+i(\frac{1}{2}\Gamma_i)}-\frac{1}{\omega-\omega_i-i(\frac{1}{2}\Gamma_i)}\right],$$
$$\hat{f}_i=\frac{C_i}{|\omega|}\tfrac{1}{2}\Gamma_i\left[\frac{1}{\omega-\omega_i+i(\frac{1}{2}\Gamma_i)}+\frac{1}{\omega+\omega_i-i(\frac{1}{2}\Gamma_i)}\right], \quad (3.9)$$

where

$$\omega_i=[(M_i^*)^2-M^2]/2M_i^*$$

are the c.m. photon resonance energies given in Table II along with the laboratory photon resonance energies

$$\omega_i^{\text{lab}}=(M_i^*/M)\omega_i.$$

The constants C_i are assumed to be real and are obtained from a fit to the proton Compton scattering data. Unitarity requires that $C_i>0$. The resonance widths are given by

$$\Gamma_i=\Gamma_{0i}\left|\frac{h}{h_i}\right|\frac{v_L(|hd|)}{v_L(|h_id|)}\theta(|\omega|-\omega_T), \quad (3.10)$$

where L is the orbital angular momentum of the ith resonance and

$$v_L^{(Z)}=[j_L^2(Z)+n_L^2(Z)]^{-1},$$

j_L and n_L being the spherical Bessel and Neumann functions of order L, respectively. The energy ω_T is the threshold photon energy in the c.m. system for pion production and is equal to 131 MeV (151 MeV in the laboratory). The factor h is the c.m. pion momentum

$$h=\{[V+(M+m_\pi)][V-(M+m_\pi)][V+(M-m_\pi)]\times[V-M-m_\pi)]\}^{1/2}/2V \quad (3.11)$$

and h_i is given by (3.11) with V replaced by M_i^*. The values of h_i for the four resonances are given in Table II. The use of the pion momentum in (3.10) ensures smooth behavior of the amplitude at the pion threshold

ω_T. Finally, the factor d is a measure of the interaction radius of the resonance. From fits to photoproduction data in the region of the $\Delta(1236)$,[21] d is found to be 1.2 F$=(160\text{ MeV})^{-1}$. We use this value for all four resonances.

The above results are combined using (3.7) and (3.3), and the proton Compton scattering cross section is computed using (3.2). The constants C_i are obtained by fitting the cross section to the experimental results at $\theta^*=65°$ [20] and $\theta^*=90°$.[22] The fits are shown in Fig. 6 and the resulting values of C_i are given in Table II. The fit in the region of the $N(1400)$ is slightly improved in Fig. 8(a) when C_2 is increased. However, because of the large width of this resonance, there is substantial interference with the higher mass resonances, causing larger values of C_2 to decrease the quality of the fit at higher energies.

IV. EXCITED INTERMEDIATE PROTON STATES

We now proceed to calculate the s-channel resonance contribution to the two-photon exchange effect. We use the resonance portion of the Compton amplitude (3.1). Since the photons in Fig. 1 are now off their mass shell, the amplitude is generalized by allowing $\omega\neq|\mathbf{k}|$. T_C in (3.1) has been obtained for the scattering of

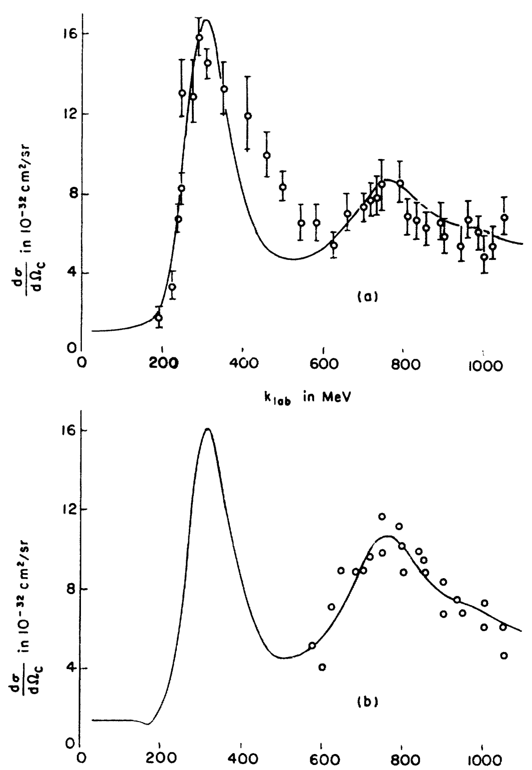

FIG. 6. Fits to the proton Compton scattering data. (a) $\theta^*=90°$ (data from Ref. 22), (b) $\theta^*=65°$ (data from Ref. 20).

[21] S. L. Adler and F. J. Gilman, Phys. Rev. **152**, 1460 (1966).
[22] D. R. Rust *et al.*, Phys. Rev. Letters **15**, 738 (1965).

transverse photons. It has been found in pion electroproduction experiments in the region of the $\Delta(1236)$ [23] that the amplitudes for longitudinal photons contribute of the order of 10% to the entire amplitude, so that the use of (3.1) is at least good as a first approximation.

The lowest-order amplitudes will again be those obtained from (2.5). As in Sec. II, however, we shall compare our results with the correct lowest-order c.m. cross section (2.7). We calculate using only the $\Delta(1236)$ contribution to (3.1). The contribution of the $N(1400)$ has been obtained elsewhere[13] and is found to be negligibly small.

The further contribution to the right-hand side of (2.8) due to the $\Delta(1236)$ is given by

$$\left(\frac{d\sigma^{(2)}}{d\Omega}\right)_c=\sigma_M\frac{\alpha}{\pi^3}\frac{M}{W}\frac{\mathbf{Q}^2}{\mathbf{P}^2}F(Q^2)(\mathrm{Re}I)\,,$$

$$\begin{aligned}I={}&\tfrac{1}{2}C_1\int_{-\infty}^{\infty}\frac{d\omega}{|\omega|^3}\int d^3q\,\frac{1}{\mathbf{q}^2-(E-\omega)^2-i\epsilon}\\&\times\frac{F(|\mathbf{q}-\mathbf{p}_f|^2-\omega^2)}{|\mathbf{q}-\mathbf{p}_f|^2-\omega^2}\frac{F(|\mathbf{q}-\mathbf{p}_i|^2-\omega^2)}{|\mathbf{q}-\mathbf{p}_i|^2-\omega^2}\\&\times\tfrac{1}{2}i\Gamma_1(\omega)\left[\left(\frac{1}{\omega-\omega_1+\frac{1}{2}i\Gamma_1}-\frac{1}{\omega+\omega_1-\frac{1}{2}i\Gamma_1}\right)n_e\right.\\&\left.+\left(\frac{1}{\omega-\omega+\frac{1}{2}i\Gamma_1}+\frac{1}{\omega+\omega_1-\frac{1}{2}i\Gamma_1}\right)n_m\right],\end{aligned}\quad(4.1)$$

$$\begin{aligned}n_e={}&-2E[\mathbf{P}^2(\mathbf{q}\cdot\mathbf{P})-2\mathbf{q}^2\mathbf{P}^2-2(\mathbf{q}\cdot\mathbf{P})^2+4\mathbf{q}^2(\mathbf{q}\cdot\mathbf{P})]\\&+(E-\omega)[\mathbf{P}^4-4\mathbf{P}^2(\mathbf{q}\cdot\mathbf{P})+4\mathbf{q}^2\mathbf{P}^2-2\mathbf{Q}^2(\mathbf{q}\cdot\mathbf{P})]\,,\end{aligned}$$

$$\begin{aligned}n_m={}&[(1+\kappa)/2W]\{8E^2\mathbf{Q}^2\mathbf{q}^2-(4E^2+\mathbf{Q}^2)(\mathbf{q}\cdot\mathbf{Q})^2\\&-4E^2\mathbf{Q}^2(\mathbf{q}\cdot\mathbf{P})+\mathbf{Q}^2(\mathbf{q}\cdot\mathbf{P})^2-2\mathbf{Q}^2\mathbf{q}^2(\mathbf{q}\cdot\mathbf{P})\\&+2E(E-\omega)[\mathbf{P}^2\mathbf{Q}^2-3\mathbf{Q}^2(\mathbf{q}\cdot\mathbf{P})+2\mathbf{Q}^2\mathbf{q}^2-2(\mathbf{q}\cdot\mathbf{Q})^2]\}\,.\end{aligned}$$

We use Yukawa form factors as in (2.12) with an rms radius of 0.8 F.[24] The details of the integration of (4.1) are given in Ref. 13. The results are shown for three c.m. energies in Fig. 7 in terms of the positron-to-electron differential cross-section ratio defined as in (2.11). The variation of the resonance contribution to the ratio at 180° is shown in Fig. 8. These results compare well with the qualitative results of Drell and Fubini[6] and the more detailed results of Campbell[8] in magnitude, sign, and angular variation.

From the results of this calculation we can conclude that although the resonance contributions to proton Compton scattering are large, their effect in e-p scattering is never greater than a few percent. This observation has been explained previously[5,6] by indicating that

[23] D. Imrie, C. Mistretta, and R. Wilson, Phys. Rev. Letters **20**, 1074 (1968).
[24] W. W. Ash *et al.*, Phys. Letters **24B**, 165 (1967); C. Mistretta *et al.*, Phys. Rev. Letters **20**, 1070 (1968).

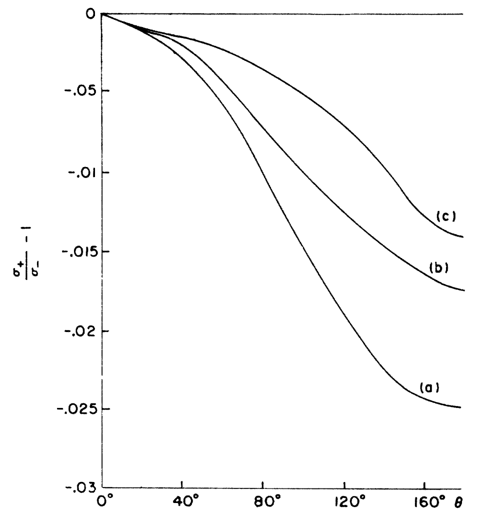

FIG. 7. The Δ(1236) contribution to e-p scattering at various c.m. energies. (a) $E=500$ MeV, (b) $E=1000$ MeV, (c) $E=2000$ MeV.

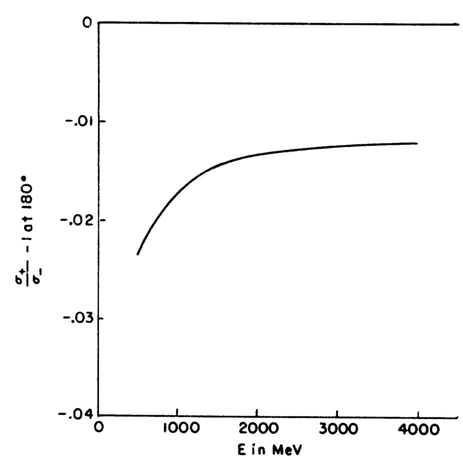

FIG. 8. The Δ(1236) contribution at 180°.

since it is the real part of the amplitude that is needed in the e-p scattering cross section, it is therefore the dispersive part of the resonance amplitude that contributes. It is argued that since this part changes sign in the region of the resonance, it contributes very little to the energy integration. However, both the absorptive and dispersive parts of the resonance amplitude contribute in (4.1), since the d^3q integration has both a real and an imaginary part. The over-all effect is small because of the factor α and because the resonance couplings appear only to first order in e-p scattering, down by one order from the proton Compton scattering cross section.

V. DISCUSSION AND CONCLUSION

By comparing the results in Figs. 3 and 7, it is seen that the second Born approximation and the resonance contributions tend to cancel one another for c.m. energies above 500 MeV. The difference in behavior between the two types of contributions is not surprising. The Δ(1236) contribution involves mainly transverse photons which undergo a p-state interaction with the proton. The proton Born-term interaction involves both transverse and longitudinal photon components with no restriction on the orbital angular momentum in the interaction.

The results given for energies above 1000 MeV are not completely justified because of the use of the static approximation. They are useful, however, as an indication of the trend to be expected for the two-photon contribution at high energies. The inclusion of the factor M/W in the magnetic moment potential (2.5a) certainly introduces some of the necessary high-energy kinematic corrections to the static model. Furthermore, despite the increase in the Born-term contribution to proton Compton scattering at high energies, the data[20] show a rapid decrease above an incident photon laboratory energy of 1100 MeV. Thus, the intermediate channels at these energies tend to cancel the effect of the Born terms and are therefore not expected to make large contributions to the two-photon exchange effect.

It should be pointed out that since we did not start from a complete expression and extract the various contributions—static potential, radiative corrections, and excited-state contributions—there may be some double counting or some small contributions omitted. However, the terms considered do seem do be physically distinct and the most likely candidates for important contributions. It should be stressed that, because of the various approximations made, it is the smallness of the over-all result that is most reliable and not the details of Figs. 3 and 7.

We can therefore conclude that because the resonant and nonresonant contributions tend to cancel at high energies, it is unlikely that the over-all contribution of two-photon exchange to $\sigma_+/\sigma_- - 1$ will exceed 2%, at least for electron energies presently available. This result is consistent with experimental data on the ratio of positron to electron scattering from protons.[2] It implies that the Rosenbluth analysis of e-p scattering[1] is valid to within a few percent, which is the accuracy of present e-p scattering experiments.[25] There is no compelling reason to improve this accuracy at this time, since we still lack a complete theoretical understanding of the over-all behavior of the nucleon form factors.[26]

ACKNOWLEDGMENT

The author would like to thank Professor Donald R. Yennie for suggesting this work and for many helpful discussions while it was in progress.

[25] D. H. Coward *et al.*, Phys. Rev. Letters **20**, 292 (1968).
[26] A. E. S. Green and T. Ueda, Phys. Rev. Letters **21**, 1499 (1968); **22**, 119 (1969).